IET Research Journals

Brief Paper

Linear LAV-based State Estimation Integrating Hybrid SCADA/PMU Measurements

A. Salehi Dobakhshari[1] S. Azizi[2] M. Abdolmaleki[3] V. Terzija[4]

[1] *Faculty of Engineering, University of Guilan, Rasht 4199613776, Iran*
[2] *School of Electronic and Electrical Engineering, University of Leeds, Leeds, LS2 9JT, U.K.*
[3] *College of Engineering and Technology, American University of the Middle East, Kuwait*
[4] *School of Electrical and Electronic Engineering, The University of Manchester, Manchester M13 9PL, U.K.*
* *E-mail: S.Azizi@leeds.ac.uk*

Abstract: The accuracy of Power System State Estimation (PSSE), its robustness against bad data and the speed of its algorithm are crucial to economic and secure system operation. On the other hand, observability and redundancy considerations mandate PSSE to take advantage of traditional SCADA measurements along with available PMU measurements. This set of hybrid PMU/SCADA inputs has traditionally made the problem formulation nonlinear, and hence time-consuming to solve due to the iterative process of solution. This paper addresses the foregoing challenges by proposing a novel linear least-absolute-value (LAV) estimation, without the need for an initial guess of the system state. The linearity of the proposed PSEE formulation is guaranteed regardless of whether PMU-only, SCADA-only or hybrid SCADA/PMU measurements are utilized. This facilitates fast and non-iterative solution of the LAV estimation of system state based on linear programming (LP). The LAV estimator outperforms the WLS estimator in dealing with erroneous measurements, by automatically rejecting bad data of any size. An extensive number of simulation studies carried out on test systems of different sizes confirm the superiorities of the proposed method in comparison with other existing PSSE methods.

1 Introduction

1.1 Motivation

Power system state estimation (PSSE) is a prerequisite for many applications in the energy management system (EMS), providing input data for economic dispatch, optimal power flow, contingency analysis, etc [1]. Many EMSs around the world still rely on measurements provided by supervisory control and data acquisition (SCADA). At the lower level of SCADA system, remote terminal units (RTUs) interface various meters to the SCADA system by transmitting telemetry data, such as voltage, active power, reactive power, circuit breaker status and other measurements to a master station. The aim of PSSE is to estimate the system state, i.e. voltage amplitude and phase-angle of network buses, using the aforementioned measurements [2].

SCADA measurements, however, are nonlinear functions of the system state and therefore PSSE has traditionally resorted to iterative algorithms such as Newton's method [3]. Currently, the weighted-least-squares (WLS) estimator is widely in use for solving PSSE with SCADA measurements as the input data [4]. There are, however, several issues related to the WLS estimator such as nonconvex nature of the problem and therefore the lack of guaranteed convergence. Besides, the sensitivity of iterative Newton's method to the starting point and post-processing of the weighted least-squares (WLS) estimation for bad data detection and identification (BDDI) needs a great deal of attention. In comparison with the WLS estimator, the LAV estimator [5] is an effective tool for solving PSSE, in the sense that it inherently counteracts the inclusion of bad data in the measurement set.

The motivations behind applying the LAV estimator to the PSSE can be summarized as follows. First, compared to magnetic instrument transformer, the accuracy of measurements is much higher in optical transformers [6]. Increasing growth of employing these transformers in substations is apt to the LAV estimation where, as will be shown in this article, the results lean toward the most accurate error-free measurements. Second, the most time-consuming procedure in WLS estimator is construction of the hat matrix [2] for bad data identification. This matrix needs to be revised once the measurement set or network topology changes. For large-scale systems, in particular, this becomes cumbersome, while the proposed LAV estimator rejects bad data automatically without a separate BDDI procedure. Third, even though LAV estimator has already been suggested for PSSE, its application, in particular to large-scale systems, has been quite limited as can be seen in the literature. This has motivated the non-iterative formulation in this article. Fourth, the conventional WLS estimator assumes perfect knowledge of impedance data and only considers error in measurements. This is not the case in practice as most utilities encounter impedance data error up to 30 % in their database [7]. The LAV estimator is expected to ignore measurements associated with these impedance data.

1.2 Literature Survey

LAV application to PSEE has been quite limited due to the computational burden of nonlinear PSSE which involves iterations [8–11].

In order to overcome the nonlinear nature of PSSE, semidefinte and conic programming have been used in [12–14] for convexication of power flow equations. The techniques introduced in [15, 16] tackle the problem by introducing redundant unknowns in order to formulate the problem linearly. Another line of research utilizes synchrophasor measurements [17] to have linear equations in the first place [18–20]. The utilization of line flow measurements has been studied since the emergence of PSSE up to recently [12, 21–25]. The formulation, however has been nonlinear, unless line measurements are provided by PMUs [26].

1.3 Contribution

In contrast to previous SCADA-based LAV estimators for PSSE, the proposed method involves no iterations thereby greatly increasing the speed of PSEE. More importantly, no approximation or constraint relaxation is required in contrast to existing convexification-based algorithms. GPS-synchronized measurements may also be incorporated in the formulation, although the proposed PSSE method is generalized in the sense that its input data do not have to be necessarily synchronized. This paves the way for integrating PMU measurements into the existing SCADA measurements in order to run a hybrid PSSE, while keeping solution process quite fast by commercial LP solvers available today. Therefore, the proposed method overcomes the difficulties of the traditional PSSE such as need for initial guess, lack of guaranteed convergence and vulnerability to bad data, while utilizing the same measurements as input data.

2 Problem Definition

The SE problem is defined as finding the most probable state of the system, i.e. voltage amplitudes and phase angles of different buses, given a set of measurements at different substations.

2.1 Assumptions

2.1.1 SCADA Measurements: Conventional SE concerns SCADA measurements updated every 2-6 seconds. It is assumed that SCADA system provides 1) voltage amplitudes of busbars, 2) active power through branches and 3) reactive power through branches. A branch refers to either a transmission line or a transformer. It should be noted that step-down transformers along with its associated downstream network may be modeled as a load. Likewise, a step-up transformer connects a generating unit to the system. In these two cases, the flow measurements of transformers are referred to as $injection\ \ measurmenents$. Accordingly, the last four above-mentioned measurements are assumed to be also available for injection measurements. These four types of measurements are assumed to have independent statistical errors, each following a Gaussian distribution with zero mean and known variance.

2.1.2 PMU Measurements: PMU-based SE envisioned for future EMSs utilizes accurate time-tagged voltage and current synchrophasor measurements updated every cycle. It is assumed that PMUs measure 1) phase angles of busbar voltages, 2) synchrophasors of busbar voltages and 3) synchrophasors of branch currents.

It is assumed that the measured magnitude and phase angle of each voltage or current synchrophasor deviates from its true value randomly. The measurement error of the magnitude and phase angle of each synchrophasor independently follows a Gaussian distribution with zero mean and known variance.

2.2 Formulation

Hybrid SE integrates a limited number of PMU measurements into the existing SCADA measurements to enhance the accuracy of estimation. Hybrid SE is quite challenging due to the unmatched refresh rate of SCADA and PMU measurements and nonlinear relationship of SCADA measurements and complex voltages among others. This paper aims to present a linear formulation for hybrid SE, including both SCADA and PMU measurements. The problem can be written as a set of linear complex equations as follows.

$$\begin{bmatrix} \left[\boldsymbol{H}^{PMU}\right] \\ \left[\boldsymbol{H}^{SCADA}\right] \end{bmatrix} \begin{bmatrix} \underline{\boldsymbol{V}} \\ e^{j\underline{\delta}} \end{bmatrix} + \begin{bmatrix} \underline{\boldsymbol{\epsilon}}^{PMU} \\ \underline{\boldsymbol{\epsilon}}^{SCADA} \end{bmatrix} = \begin{bmatrix} \underline{\boldsymbol{z}}^{PMU} \\ \underline{\boldsymbol{z}}^{SCADA} \end{bmatrix} \tag{1}$$

where H and z denote known coefficient matrix and measurement vector, respectively. $\underline{V}$ and $e^{j\underline{\delta}}$ denote unknown vectors of bus voltage phasors and phase-angles, respectively. $\underline{\boldsymbol{\epsilon}}$ denotes the vector of measurement errors, whose expected value and covariance matrix are attainable and therefore known.

The above formulation for hybrid SE differs from previous methods in several ways. First, it is linear. Second, it includes additional redundant states reflected as $e^{j\underline{\delta}}$, which is the vector of voltage phase-angles with respect to the reference bus. Third, it will be shown that while $\left[H^{PMU}\right]$ is a constant matrix composed of network parameters, $\left[H^{SCADA}\right]$ includes not only fixed network parameters, but also measurements.

In what follows, known matrices and vectors employed in (1) will be presented in detail.

2.3 Notations

The formulation presented includes real- and complex-valued vectors and matrices.

V_k	Real-valued voltage magnitude at bus k
$\boldsymbol{V}_k$	Complex-valued voltage phasor at bus k
$.^{meas}$ and $.^{true}$	Measured and true quantities
$\varepsilon.$	Real-valued measurement error defined as $.^{meas} - .^{true}$
$\boldsymbol{\epsilon}$	Complex-valued measurement error expressed in terms of different ε's
$\underline{.}$	A $v \times 1$ vector
$[.]$	A matrix
$[.]_n$	An $n \times n$ matrix
$[.]_{m\times n}$	An $m \times n$ matrix
$[(\underline{.})]$	A $v \times v$ diagonal matrix with elements of $\underline{.}_{v\times 1}$
$[I]_n$	The $n \times n$ identity matrix
$\underline{0}$	A $v \times 1$ vector with zero elements
$[0]_{p\times q}$	A $p \times q$ matrix with zero elements
$\underline{v}_1.\underline{v}_2$	Element-by-element product of vectors $\underline{v}_1$ and $\underline{v}_2$, i.e. $(\underline{v}_1.\underline{v}_2)_k = v_{1k}v_{2k}$

3 Modeling PMU Measurements

3.1 Phase-angle Measurements

PMUs are able to measure bus voltage phase angle, bus voltage synchrophasor and branch current synchrpphasor, all with respect to the phase angle of voltage at the reference bus. The vector of phase-angle measurements of voltages can be related to the true vector of phase angles as

$$\underline{\delta}^{meas} = \underline{\delta}^{true} + \underline{\varepsilon}_{\delta} \tag{2}$$

which can be rewritten as

$$e^{j\underline{\delta}^{meas}} = e^{j\underline{\delta}^{true}} + je^{j\underline{\delta}^{true}}.\underline{\varepsilon}_{\delta} \tag{3}$$

where . denotes element-by-element product of two vectors. Equation (3) is expressed in standard form as

$$e^{j\underline{\delta}^{meas}} = e^{j\underline{\delta}^{true}} + \underline{\boldsymbol{\epsilon}}_{\delta} \tag{4}$$

Provided that the elements of $\underline{\varepsilon}_{\delta}$ have zero mean, it is straightforward to show that the mean and variance of $\underline{\varepsilon}_{\delta}$ and $\underline{\boldsymbol{\epsilon}}_{\delta}$ are the same.

3.2 Synchrophasor Measurements of Voltages

Phasor measurement of voltages can be written as

$$\underline{\boldsymbol{V}}^{meas} = \underline{\boldsymbol{V}}^{true} + \underline{\boldsymbol{\epsilon}}_{\boldsymbol{V}} \tag{5}$$

where $\boldsymbol{\epsilon}_{\boldsymbol{V}}$ is a zero-mean vector whose variance may be calculated according to the variances of voltage phase-angle and magnitude measurements [27].

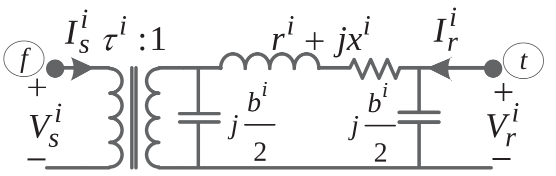

Fig. 1: General pi model for transmission lines and transformers

3.3 Synchrophasor Measurements of Currents

Let us consider branch i connecting nodes f and t, as shown in Fig. 1. From circuit equations we have

$$\begin{bmatrix} I_s^i \\ I_r^i \end{bmatrix} = \begin{bmatrix} y_{ss}^i & y_{sr}^i \\ y_{rs}^i & y_{rr}^i \end{bmatrix} \begin{bmatrix} V_s^i \\ V_r^i \end{bmatrix} \tag{6}$$

where y_{ss}^i, y_{sr}^i, y_{rs}^i and y_{rr}^i are obtained by the circuit equations. If the branch is a transmission line, the tap ratio of the transformer (τ^i) will be 1. If the branch is a transformer, then the shunt susceptance (b_i) will be zero.

Based on (6), the vectors of sending- and receiving-end currents can be obtained as

$$\underline{I}_s = [Y_s]\,\underline{V} \tag{7}$$

$$\underline{I}_r = [Y_r]\,\underline{V} \tag{8}$$

where $[Y_s]$ and $[Y_r]$ are built as follows.

$$[Y_s] = [\underline{Y}_{ss}]\,[A_s] + [\underline{Y}_{sr}]\,[A_r] \tag{9}$$

$$[Y_r] = [\underline{Y}_{rs}]\,[A_s] + [\underline{Y}_{rr}]\,[A_r] \tag{10}$$

where $[\underline{Y}_{ss}]$, $[\underline{Y}_{sr}]$, $[\underline{Y}_{rs}]$ and $[\underline{Y}_{rr}]$ are diagonal matrices, whose $(i,i)^{th}$ elements comprise of corresponding elements of (6). $[A_s]$ and $[A_r]$ are respectively sending- and receiving-end connectivity sparse matrices. That is, the $(i,f)^{th}$ element of $[A_s]$ and the $(i,t)^{th}$ element of $[A_r]$ are equal to 1 for each branch i that connects nodes f and t, as shown in Fig. 1.

The vector of branch synchrophasor currents can therefore be written as

$$\begin{bmatrix} \underline{\boldsymbol{I_s}}^{meas} \\ \underline{\boldsymbol{I_r}}^{meas} \end{bmatrix} = \begin{bmatrix} [Y_s] \\ [Y_r] \end{bmatrix} \underline{\boldsymbol{V}}^{true} + \begin{bmatrix} \boldsymbol{\epsilon_{I_s}} \\ \boldsymbol{\epsilon_{I_r}} \end{bmatrix} \tag{11}$$

3.4 State Estimation by Synchrophasor Measurements

Equations (4), (5) and (11) may be combined to formulate the PMU-based SE as follows:

$$\begin{bmatrix} [0]_{(n-1)\times n} & [I]_{n-1} \\ [I]_n & [0]_{n\times(n-1)} \\ [Y_s]_{m\times n} & [0]_{m\times(n-1)} \\ [Y_r]_{m\times n} & [0]_{m\times(n-1)} \end{bmatrix} \begin{bmatrix} \underline{\boldsymbol{V}} \\ e^{j\underline{\delta}} \end{bmatrix} + \boldsymbol{\epsilon} = \begin{bmatrix} e^{j\underline{\delta}^{meas}} \\ \underline{\boldsymbol{V}}^{meas} \\ \underline{\boldsymbol{I}_s}^{meas} \\ \underline{\boldsymbol{I}_r}^{meas} \end{bmatrix} \tag{12}$$

It is worth noting that $\left[H^{PMU}\right]$ and $\underline{z}^{PMU}$ in the first line of (1) can be distinguished in (12). Variants of (12) can be seen in the previous literature on PMU-only SE, probably with the exception of the first line, where phase-angle measurements are directly used. This owes to the redundant state variables introduced in this paper aiming at a unified linear formulation in presence of both SCADA and PMU measurements.

4 Modeling SCADA Measurements

4.1 Measurements of Bus Voltage Amplitudes

The vector of voltage amplitude measurements can be related to the true vector of voltage amplitude as

$$\underline{V}^{meas} = \underline{V}^{true} + \underline{\varepsilon}_V \tag{13}$$

where $\underline{\varepsilon}_V$ is characterized by the accuracy level of meters. Element-wise Multiplication of both sides by $e^{j\underline{\delta}^{true}}$ leads to expression of voltage amplitude measurements in terms of complex bus voltages as follows:

$$\underline{V}^{meas}.e^{j\underline{\delta}^{true}} = \underline{\boldsymbol{V}}^{true} + \underline{\varepsilon}_V.e^{j\underline{\delta}^{true}} \tag{14}$$

which can be rewritten as

$$\left[\left(\underline{V}^{meas}\right)\right] e^{j\underline{\delta}^{true}} = \underline{\boldsymbol{V}}^{true} + \boldsymbol{\epsilon_V} \tag{15}$$

It can be shown from (14) and (15) that $\boldsymbol{\epsilon_V}$ and $\underline{\varepsilon}_V$ have the same mean and variance values.

4.2 Measurements of Branch Current Phasors

Provided that $\boldsymbol{V}_s^i = V_s^i\measuredangle\delta_s^i$ and $\boldsymbol{I}_s^i = I_s^i\measuredangle\theta_s^i$ then active and reactive power flows through branch i can be written as

$$P_s^i = V_s^i I_s^i cos(\delta_s^i - \theta_s^i) \tag{16}$$

$$Q_s^i = V_s^i I_s^i sin(\delta_s^i - \theta_s^i) \tag{17}$$

which yields

$$\theta_s^i = \delta_s^i + tg^{-1}(-\frac{Q_s^i}{P_s^i}) \tag{18}$$

Therefore, complex branch current can be written as

$$\boldsymbol{I}_s^i = I_s^i e^{j\theta_s^i} = \left(I_s^i e^{jtg^{-1}(-\frac{Q_s^i}{P_s^i})}\right) e^{j\delta_s^i} \tag{19}$$

where I_s^i may be calculated by measured quantities as

$$I_s^i = \frac{\sqrt{{P_s^i}^2 + {Q_s^i}^2}}{V_s^i} \tag{20}$$

It should be noted that SCADA measurements contain V_s^i, P_s^i and Q_s^i. Substituting (7) into (19) we have

$$\left((\underline{I}_s^{meas} - \underline{\varepsilon}_{I_s}).e^{jtg^{-1}(-\frac{\underline{Q}_s^{meas} - \underline{\varepsilon}_{Q_s}}{\underline{P}_s^{meas} - \underline{\varepsilon}_{P_s}})}\right).e^{j\underline{\delta}_s^{true}} = [Y_s]\,\underline{\boldsymbol{V}}^{true} \tag{21}$$

which can be rewritten as

$$\left(\underline{I}_s^{meas}.e^{jtg^{-1}(-\frac{\underline{Q}_s^{meas}}{\underline{P}_s^{meas}})} - \boldsymbol{\varepsilon_{I_s}}\right).e^{j\underline{\delta}_s^{true}} = [Y_s]\,\underline{\boldsymbol{V}}^{true} \tag{22}$$

To write in a standard form, (22) can be expressed as

$$\left(\underline{I}_s^{meas}.e^{jtg^{-1}(-\frac{\underline{Q}_s^{meas}}{\underline{P}_s^{meas}})}\right).e^{j\underline{\delta}_s^{true}} - \boldsymbol{\epsilon_{I_s}} = [Y_s]\,\underline{\boldsymbol{V}}^{true} \tag{23}$$

And in terms of state variables we have

$$\left[\left(\underline{I}_s^{meas}.e^{jtg^{-1}(-\frac{\underline{Q}_s^{meas}}{\underline{P}_s^{meas}})}\right)\right][A_s]\,e^{j\underline{\delta}^{true}} - \boldsymbol{\epsilon_{I_s}} = [Y_s]\,\underline{\boldsymbol{V}}^{true} \tag{24}$$

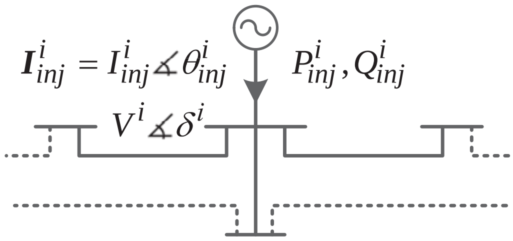

Fig. 2: Modeling Injection Measurements

Similarly, for the receiving-end currents we have

$$\left[\left(\underline{I}_r^{meas}.e^{jtg^{-1}(-\frac{Q_r^{meas}}{P_r^{meas}})}\right)\right][A_r]\,e^{j\underline{\delta}^{true}} - \underline{\boldsymbol{\epsilon}}_{\boldsymbol{I_r}} = [Y_r]\,\underline{\boldsymbol{V}}^{true} \tag{25}$$

It should be noted that $\underline{I}_s^{meas}.e^{jtg^{-1}(-\frac{Q_s^{meas}}{P_s^{meas}})}$ and $\underline{I}_r^{meas}.e^{jtg^{-1}(-\frac{Q_r^{meas}}{P_r^{meas}})}$ are branch current phasors, expressed in terms of SCADA measurements, provided that current amplitude measurements are telemetered to the control center. However, these current phasors are not synchrophasors as they are not expressed with respect to a common phase-angle reference. Therefore, there is no need for the GPS signal for linear expression of SCADA measurements in (24) and (25).

4.3 Injection Measurements

Injection currents, either by generators or loads, may be related to complex voltages of the network through bus-admittance matrix. This is simply expressed in matrix form as

$$\underline{I}_{inj} = [Y_{bus}]\,\underline{V} \tag{26}$$

Although the injection measurements often comprise of injected active and reactive powers, the injected current amplitude can also be telemetered by SCADA. A procedure similar to (16)-(18) can be followed based on Fig. 2 to express the complex injected current as:

$$\boldsymbol{I}^i_{inj} = I^i_{inj} e^{j\theta^i_{inj}} = \left(I^i_{inj} e^{jtg^{-1}(-\frac{Q^i_{inj}}{P^i_{inj}})}\right) e^{j\delta^i} \tag{27}$$

where superscript i refers to the injection bus and I^i_{inj} is calculated by

$$I^i_{inj} = \frac{\sqrt{{P^i_{inj}}^2 + {Q^i_{inj}}^2}}{V_i} \tag{28}$$

Substituting (27) into (26) we have

$$\left((\underline{I}_{inj}^{meas} - \varepsilon_{I_{inj}}).e^{jtg^{-1}(-\frac{Q_{inj}^{meas} - \varepsilon_{Q_{inj}}}{P_{inj}^{meas} - \varepsilon_{P_{inj}}})}\right).e^{j\underline{\delta}^{true}} = [Y_{bus}]\,\underline{\boldsymbol{V}}^{true} \tag{29}$$

It is worth noting that the obtained equation resembles (21). A similar procedure is therefore followed to write:

$$\left[\left(\underline{I}_{inj}^{meas}.e^{jtg^{-1}(-\frac{Q_{inj}^{meas}}{P_{inj}^{meas}})}\right)\right] e^{j\underline{\delta}^{true}} - \underline{\boldsymbol{\epsilon}}_{\boldsymbol{I_{inj}}} = [Y_{bus}]\,\underline{\boldsymbol{V}}^{true} \tag{30}$$

4.4 State Estimation by SCADA Measurements

Equations (15), (24), (25) and (30) may be integrated as a system of linear equations as follows.

$$\begin{bmatrix} [I]_n & \begin{matrix}[0]_{1\times(n-1)} \\ [-\underline{V}^{meas} \setminus V_1^{meas}]_{n-1}\end{matrix} \\ [Y_s]_{m\times n} & \begin{matrix}[0]_{n_s^1\times(n-1)} \\ -\left[\underline{\hat{\boldsymbol{I}}}_{\boldsymbol{s}}{}^{meas}\right]_{m-n_s^1}\left[\hat{A}_s\right]_{(m-n_s^1)\times(n-1)}\end{matrix} \\ [Y_r]_{m\times n} & \begin{matrix}[0]_{n_r^1\times(n-1)} \\ -\left[\underline{\hat{\boldsymbol{I}}}_{\boldsymbol{r}}{}^{meas}\right]_{m-n_r^1}\left[\hat{A}_r\right]_{(m-n_r^1)\times(n-1)}\end{matrix} \\ [Y_{bus}]_{n\times n} & \begin{matrix}[0]_{1\times(n-1)} \\ -\left[\underline{\hat{\boldsymbol{I}}}_{\boldsymbol{inj}}{}^{meas}\right]_{(n-1)\times(n-1)}\end{matrix} \end{bmatrix} \begin{bmatrix} V_1 \\ \underline{\hat{\boldsymbol{V}}} \\ e^{j\underline{\delta}} \end{bmatrix}_{(2n-1)\times 1} + \underline{\boldsymbol{\epsilon}} = \begin{bmatrix} V_1^{meas} \\ \underline{0}_{(n-1)\times 1} \\ \underline{\hat{\boldsymbol{I}}}_{\boldsymbol{s1}}{}^{meas} \\ \underline{0} \\ \underline{\hat{\boldsymbol{I}}}_{\boldsymbol{r1}}{}^{meas} \\ \underline{0} \\ \boldsymbol{I}_{inj,1}^{meas} \\ \underline{0} \end{bmatrix} \tag{31}$$

Let us go through (31) in detail and clarify its derivation from (15), (24), (25) and (30) one by one.

4.4.1 Voltage Amplitude Measurements: There is a distinction between voltage at the reference bus (real-valued voltage V_1) and the vector of complex voltages at other buses ($\underline{\hat{\boldsymbol{V}}}$) in the state vector. By definition, we know that the phase angle of V_1 is zero and any other voltage at bus k, $k = 2, 3, ..., n$, is expressed as $\boldsymbol{V}_k = V_k e^{j\delta_k}$. The first row of (31) reflects the measurement of bus voltage at the reference bus (bus 1). The other n-1 rows reflect bus voltage measurements at other buses. It should be noted that $\underline{V}^{meas} \setminus V_1^{meas}$ denotes the real-valued vector $[V_2^{meas}, ..., V_n^{meas}]^T$ and it is recalled that $[\underline{V}]$ denotes a diagonal matrix whose elements are those in vector $\underline{V}$. Accordingly, the first n rows in (31) are a rephrased version of (15).

4.4.2 Branch Current Measurements: It is assumed that there are sending-end measurements from m branches in the network. To save space, we define $\underline{\hat{\boldsymbol{I}}}_{\boldsymbol{s}}{}^{meas} \triangleq \underline{I}_s^{meas}.e^{jtg^{-1}(-\frac{Q_s^{meas}}{P_s^{meas}})}$. There is a distinction made between branches whose sending-end bus is the reference bus and other branches. $\underline{\hat{\boldsymbol{I}}}_{\boldsymbol{s1}}{}^{meas}$ and $\underline{\hat{\boldsymbol{I}}}_{\boldsymbol{s}}{}^{meas}$ in the RHS and LHS of (31) denote the vectors of branch current measurements associated with these two sets, respectively. n_s^1 is the number of branches whose sending-end bus is the reference bus. That is, according to Fig. 1:

$$n_s^1 = |\{i = (f, t) | f = 1\}| \tag{32}$$

$\left[\hat{A}_s\right]$ is the sending-end connectivity matrix for branches whose sending end is not bus 1. This matrix is obtained from $[A_s]$ in (9) by removing the n_s^1 rows related to bus 1 in $[A_s]$.

m rows are therefore devoted in (31) to branch current measurements according to (24). The difference is that since $\delta_1 = 0$ in (24) by definition, $\underline{\hat{\boldsymbol{I}}}_{\boldsymbol{s}}{}^{meas}$ in (24) is partitioned into two vectors of $\underline{\hat{\boldsymbol{I}}}_{\boldsymbol{s1}}{}^{meas}$ and $\underline{\hat{\boldsymbol{I}}}_{\boldsymbol{s}}{}^{meas}$. Receiving-end currents are treated similarly, assuming that current amplitudes and active and reactive power flows at both ends of the m branches are measured.

4.4.3 Injection Measurements: Injection measurements are treated very much like branch current measurements. It is assumed that there are n injection measurements at all buses. The vector of injection measurements $\underline{\hat{\boldsymbol{I}}}_{\boldsymbol{inj}}{}^{meas} \triangleq \underline{I}_{inj}^{meas}.e^{jtg^{-1}(-\frac{Q_{inj}^{meas}}{P_{inj}^{meas}})}$ in (30) is partitioned into the injection measurement at the reference bus, i.e. $\boldsymbol{I}_{inj,1}^{meas}$, and the vector of injection measurements at buses $2, ..., n$, i.e. $\underline{\hat{\boldsymbol{I}}}_{\boldsymbol{inj}}{}^{meas}$. It is straightforward to show that the last n rows of (31) is rephrasing (30).

5 Hybrid Linear LAV Estimator

Equation (31) can be appended to (12) in order to form (1). It is worth noting that $\left[H^{PMU}\right]$, $\underline{\boldsymbol{\epsilon}}^{PMU}$ and $\underline{z}^{PMU}$ are presented in

(12), while $\left[H^{SCADA}\right]$, $\underline{\boldsymbol{\epsilon}}^{SCADA}$ and $\underline{z}^{SCADA}$ can be seen in (31). Equation (1) can be rewritten as a system of linear equations as follows.

$$[\boldsymbol{H}]\left[\begin{array}{c}\underline{\boldsymbol{V}}\\ e^{j\underline{\delta}}\end{array}\right]+\underline{\boldsymbol{\epsilon}}=\underline{\boldsymbol{z}} \tag{33}$$

where $[\boldsymbol{H}]$ is of size $(4m+4n-1)\times(2n-1)$ while $\underline{\boldsymbol{\epsilon}}$ and $\underline{\boldsymbol{z}}$ are of size $(4m+4n-1)\times 1$. Theorem 1 helps solve (33), optimally.

5.1 Robust Estimation of Voltage Phase Angles

It is evident from (33) that no constraint is imposed on the amplitude of $e^{j\delta_i}$, which is 1. Otherwise, the problem would be nonlinear again. To resolve this issue, the idea is to solve the problem in two steps: first, the phase-angle variables are estimated while preserving the linear structure of formulation. Next, the estimated phase angles can be used to estimate the system state by another reduced linear system of equations. The first problem is dealt with here while the next will be solved in the subsequent subsection.

Separating (33) into real and imaginary parts yields

$$\left[\begin{array}{cc}\left[H^R\right] & \left[-H^I\right]\\ \left[H^I\right] & \left[H^R\right]\end{array}\right]\left[\begin{array}{c}\underline{x}^R\\ \underline{x}^I\end{array}\right]+\left[\begin{array}{c}\underline{\varepsilon}^R\\ \underline{\varepsilon}^I\end{array}\right]=\left[\begin{array}{c}\underline{z}^R\\ \underline{z}^I\end{array}\right] \tag{34}$$

where $(.)^R$ and $(.)^I$ denote the real and imaginary parts of the complex argument, respectively. In a compact form, this real-valued system of equations is written as

$$[M]\underline{y}+\underline{r}=\underline{b} \tag{35}$$

The unknown vector obtained by an LAV estimator is comprised of

$$\begin{array}{rl} y= & [V_1\ V_2cos\delta_2\ ...\ V_ncos\delta_n\ cos\delta_2\ ...\ cos\delta_n\\ & V_2sin\delta_2\ ...\ V_nsin\delta_n\ sin\delta_2\ ...\ sin\delta_n]^T\end{array} \tag{36}$$

Least absolute value (LAV) estimation of $\underline{y}$ minimizes sum of the absolute of residuals

$$\begin{array}{ll}\underset{y}{Min}\ \|\underline{r}\|_1 & \\ s.t. \quad \underline{r}=\underline{b}-[M]\underline{y} & \end{array} \tag{37}$$

An equivalent linear programming (LP) problem for (37) can be defined as [5]

$$\begin{array}{l}\underset{y}{Min}\ \underline{f}^T\underline{r}\\ s.t.\quad \left[\begin{array}{cc}[-M] & [-I]\\ [M] & [-I]\end{array}\right]\left[\begin{array}{c}\underline{y}\\ \underline{r}\end{array}\right]\le\left[\begin{array}{c}-\underline{b}\\ \underline{b}\end{array}\right]\end{array} \tag{38}$$

where f may consist of identical non-zero elements (LAV estimator) or the the inverse of the standard deviation of the associated meter (WLAV estimator). The LP problem in (38) can be rewritten in matrix form as

$$\begin{array}{l}\underset{y}{Min}\ \underline{w}^T\underline{u}\\ s.t.\quad [B]\,\underline{u}\le\underline{v}\end{array} \tag{39}$$

where

$$\begin{array}{l}\underline{w}=\left[\underline{0}\quad \underline{f}\right]^T\\ \underline{u}=\left[\underline{y}\quad \underline{r}\right]^T\\ \underline{v}=\left[-\underline{b}\quad \underline{b}\right]^T\end{array} \tag{40}$$

Existing LP solvers are able to solve (39), efficiently. Once (39) is solved, voltage phase-angles may be estimated robustly by

$$\hat{\delta}_i=tg^{-1}\frac{\widehat{sin\delta_i}}{\widehat{cos\delta_i}} \tag{41}$$

where $\widehat{sin\delta_i}$ and $\widehat{cos\delta_i}$ are the elements of $\underline{u}$, obtained by the LAV estimator.

5.2 Linear LAV Estimator Using Estimated Phase Angles

Once the phase angles of complex voltages at all buses are calculated from (41), it is possible to formulate the problem as another linear LAV estimation, aiming at estimating the bus voltage amplitudes. This is achieved by putting all the voltage and current measurements in (31) in the measurement vector as below.

$$\left[\begin{array}{c}[I]_n\\ [Y_s]_{m\times n}\\ [Y_r]_{m\times n}\\ [I]_n\\ [Y_s]_{m\times n}\\ [Y_r]_{m\times n}\\ [Y_{bus}]_{n\times n}\end{array}\right][\underline{\boldsymbol{V}}]+\underline{\boldsymbol{\epsilon}}=\left[\begin{array}{c}\underline{\boldsymbol{V}}^{meas}\\ \underline{\boldsymbol{I}_s}^{meas}\\ \underline{\boldsymbol{I}_r}^{meas}\\ \left[e^{j\underline{\hat{\delta}}}\right]\left[\underline{V}^{meas}\right]\\ \left[e^{j\underline{\hat{\delta}}}\right]\left[\underline{\hat{\boldsymbol{I}}_s}^{meas}\right][A_s]\\ \left[e^{j\underline{\hat{\delta}}}\right]\left[\underline{\hat{\boldsymbol{I}}_r}^{meas}\right][A_r]\\ \left[e^{j\underline{\hat{\delta}}}\right]\left[\underline{\hat{\boldsymbol{I}}_{inj}}^{meas}\right]\end{array}\right] \tag{42}$$

where $\left[e^{j\underline{\hat{\delta}}}\right]$ is a diagonal matrix containing $e^{j\hat{\delta}_i}$ values solved in (41). It should be noted that (42) is the combination of (12) and (31), except that thanks to the phase-angle estimates in (41), the unknown terms associated with the phase angles have become known and moved to the right-hand side. Only the first three lines of (42) are related to PMU measurements and other lines are comprised of SCADA measurements.

After separating the real and imaginary parts of (42) it can be transformed into a real-valued system of linear equations as

$$[G]\underline{p}+\underline{s}=\underline{q} \tag{43}$$

where

$$\underline{p}=[V_1\ V_2cos\delta_2\ ...\ V_ncos\delta_n\ V_2sin\delta_2\ ...\ V_nsin\delta_n]^T \tag{44}$$

It is worth noting that (43) is similar to (35) and hence the same process may be followed to solve it by an LAV estimator. Another LP problem may be developed to minimize the sum of absolute errors in (43). Once (43) is solved by the LAV estimator, unknown states of the system are attainable from the elements of $\underline{p}$ as

$$\hat{V}_i=\sqrt{\hat{p}_i^2+\hat{p}_{n+i}^2} \tag{45}$$

$$\hat{\delta}_i=tg^{-1}\frac{\hat{p}_i}{\hat{p}_{n+i}} \tag{46}$$

for i=2,...,n. The estimated values are robust to measurement errors thanks to the LAV estimator, which is capable of rejecting outliers, automatically [5]. Moreover, with the advent of computer processors, the LP-based LAV estimators used here are run very fast even for large-scale problems. As a final note, in contrast to some of previous methods, no assumption regarding the network condition is required and there is no approximation when modeling the PSSE problem as an LP problem.

6 Case Studies

In this section, the proposed linear LAV state estimator is tested by more than 10000 simulations. The proposed estimator is compared with the conventional iterative WLS estimator based on Gauss-Newton algorithm [2]. The performance index used for comparison is the root-mean-square error (RMSE) defined as

$$\text{RMSE}=\sqrt{\frac{\sum_{i=1}^{n}|\hat{\boldsymbol{V}}_i-\boldsymbol{V}_i|^2}{n}}. \tag{47}$$

where $\hat{\boldsymbol{V}}_{\boldsymbol{i}}=\hat{V}_ie^{j\hat{\delta}_i}$ is the estimated complex voltage at bus i obtained by (45) and (46). In practice, the true complex voltages

Table 1 Average of RMSE for Different Systems

System	WLS	LAV
9-bus	0.00526	0.00048
14-bus	0.00564	0.00047
30-bus	0.00636	0.00065
57-bus	0.02138	0.00121
118-bus	0.00481	0.00065
300-bus	0.01742	0.00652
1354-bus	0.00719	0.00042

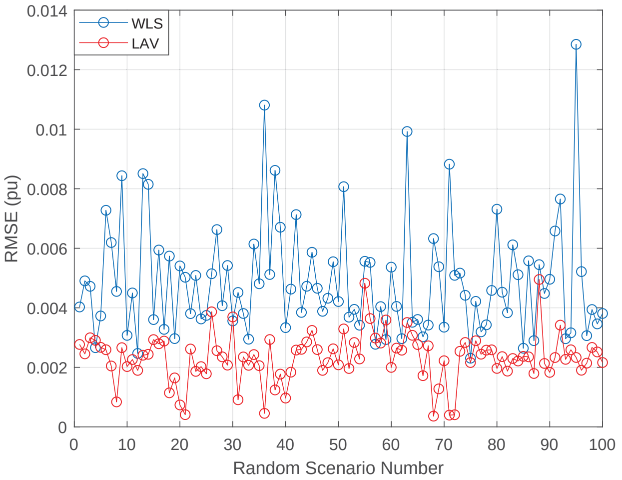

Fig. 3: LAV versus WLS estimator (Flow measurements from one end).

V_i are never known. Fortunately, this is not the case in a simulation environment, where true V_i values are simulated as the output of the load flow function in MATPOWER [28].

RMSE for the LAV estimator is tested on the IEEE 118-bus test system [29]. Voltage and flow measurement errors are assumed to be Gaussian with zero mean and the standard deviations of 0.001 pu and 0.002 pu, respectively. To generate bad data, 20$\%$ of randomly chosen branch flows have been polluted by Gaussian noise with zero mean and standard deviation of 0.1 pu. Fig. 3 reflects the results of 100 Monte Carlo simulations, where voltage amplitudes at all buses and active and reactive power flows from one end of each line are available. In Fig. 4, it is assumed that active and reactive power flows from both ends of each line are available. The WLS estimator utilizing Gauss-Newton algorithm is available in MATPOWER ($doSE.m$) [28]. Table II shows the estimation results for other IEEE test systems. It can be observed that similar to Figs. 3 and 4, the LAV estimator outperforms the WLS estimator in presence of bad data. The reason, as expected, is the robustness of the LAV estimator against outliers, while the WLS estimator leans toward bad data [5].

A comparison is made between the solution time of the proposed method, conventional method [2] and the SOCP algorithm in [12], whose results are reflected in Table 2. The conventional and proposed methods have been implemented on a PC with Core i5 8250U CPU at 1.6 GHz and 8 GB of RAM. The results of [12] are directly reported, where a Windows system with 2.7 GHz CPU and 8GB RAM is used except for the last system for which a macOS system with 2.2 GHz CPU and 12 GB RAM is utilized. It can be seen that for small- and medium-scale systems the proposed method is much faster than [12], while for large-scale systems the solution time is comparable. The linear nature of the proposed method along with efficient interior-point algorithm for solving large-scale LP problems makes the proposed algorithm superior in terms of computational burden.

Fig. 5 compares LAV and WLS estimators in terms of their corresponding average of RMSE for 1000 Monte-Carlo simulations

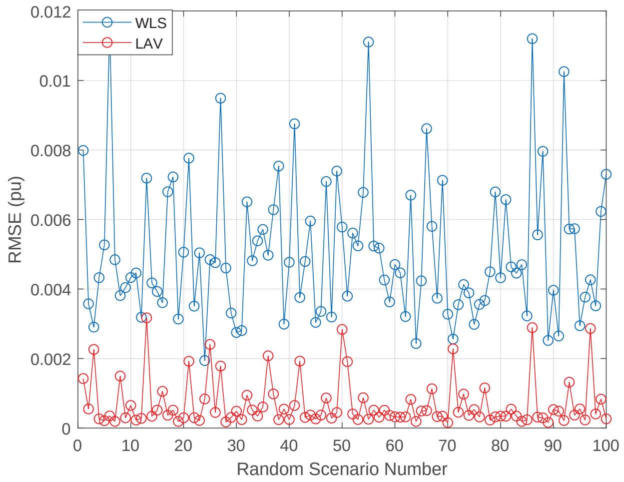

Fig. 4: LAV versus WLS estimator (Flow measurements from both ends)

Table 2 Solution time of State Estimation (in seconds) for Different Systems

System	Convexified LAV [12]	Linear LAV
9-bus	1.58	0.021
14-bus	2.54	0.034
30-bus	3.21	0.08
57-bus	4.09	0.16
118-bus	5.63	0.44
300-bus	NA	2.56
1354-bus	9.48	11.32
9241-bus	109.14	89.93

when erroneous measurements are deviated from their true values by 20$\%$. Sensitivity analysis on the percentage of bad data in the measurements has also been carried out, in conditions where erroneous measurements comprise 1$\%$ up to 20 $\%$ of total measurements. In addition, sensitivity analysis on the measurement accuracy level related to good data (σ) is carried out (x-axis). The less the ratio of $RMSE_{LAV}/RMSE_{WLS}$, the better is the performance of LAV estimator. It can be seen form sensitivity analysis that when bad data deviate from their true values significantly, the LAV estimator outperforms the WLS estimator. It can be seen that the LAV estimator is effective the most when the percentage of bad data compared to good data are high. Accordingly, the LAV estimator shows its robustness compared with WLS, when 10 to 20 $\%$ of measurements are corrupted with bad data. It should be noted that the LAV estimator outperforms WLS estimator in all conditions as the $RMSE_{LAV}/RMSE_{WLS}$ is less than 1 for all cases.

7 Discussion

The LAV state estimator essentially ignores bad data and hence rejects them automatically. The WLS estimator, however, needs bad data detection and identification (BDDI) carried out usually be largest normalized residual test (LNRT) [2].LNRT requires the computationally expensive [2] construction of Hat matrix, which depends on measurement set and network topology. Moreover, an exact BDDI requires calculating the normalized residuals, removing the erroneous measurement with the largest normalized residual and running SE again. Therefore, the WLS estimator has to be run $b+1$ times where b is the number of erroneous measurements. Therefore, if the system is prone to bad data, LAV estimator can be efficient since no hat matrix is required. Furthermore, if there are several erroneous measurements, the LAV estimator becomes faster than the

IET Research Journals, pp. 1–8

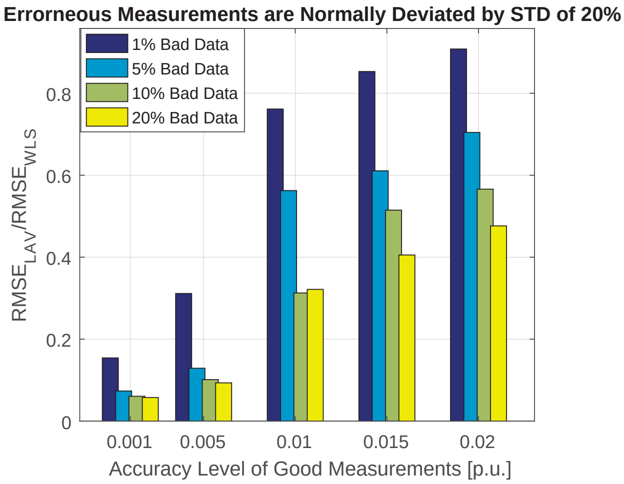

Fig. 5: LAV versus WLS estimator

WLS estimator, since its solution time is independent of the number of bad data.

Technical shortcomings and challenges of the LNRT for BDDI in the WLS estimator are briefly discussed here. The first challenge is the dependency of measurement errors. That is, for example, active and reactive power measurements are processed with inputs from voltage and current transformers. Therefore, an erroneous voltage transformer output spreads over active and reactive power measurements [30]. In addition, several good measurements may be removed along with the bad one if traditional LNRT is employed [30].

The second shortcoming is the incapability of LNRT in identifying bad data in certain conditions [31]. A single erroneous leverage point even with gross error is unlikely to be identified by LNRT. Moreover, a group of interacting leverage points also may remain undetected by LNRT. It is shown that these leverage point may account for more than a third of the total measurements [31]. It should be noted that these problems occur even when the measurement redundancy is reasonable. Otherwise, if critical measurements are erroneous, the LNRT will not be able to identify them [2].

The third challenge is the assumptions of the WLS estimator, where network parameters are assumed to be known exactly. However, in practice most of the impedances are approximate values with accuracy levels comparable to those of measurements. Most utilities are reported to include impedance data in their database with up to 25% error compared to their real vlues [7]. The complications of LNRT in WLS estimator make that estimator quite vulnerable to cyber attacks on power systems, most notably false data injection attacks [32].

8 Conclusion

A robust linear LAV estimator has been presented in this article to deal with rejection of bad data in power system state estimation. In contrast to previous robust state estimators, the proposed algorithm is generalised in the sense that either SCADA or synchrophasor measurements or a combination of both can be used as input data. The proposed estimator is linear with no approximation, which renders its solution process non-iterative. As opposed to the iteration-based algorithms requiring an update of the Jacobian matrix after each iteration, the proposed method requires only two LP problems to be solved.

The WLS estimator needs constructing the computationally expensive hat matrix and to be run for each erroneous measurement separately, if it is successful in dealing with multiple erroneous measurements. In contrast, the proposed estimator automatically rejects bad data, which is advantageous over the WLS estimator in practice, in terms of the computational effort.

Simulation results indicate that the proposed LAV estimator outperforms the conventional WLS estimator in terms of accuracy. That is if bad data is not removed from the measurement set, the proposed estimator leads to more accurate estimates than the WLS estimator. This roots in the objective function of the LAV estimation, which is optimized by ignoring the erroneous measurements while the WLS estimator leans toward bad data in order to minimize the sum of squared errors. In particular as the accuracy of meters increases, the LAV estimation results can be more than 10 times as accurate as the WLS estimator when there is gross error in a few measurements. This feature is especially attractive for large-scale state estimation, without the concern over dealing with multiple bad data.

9 References

1 Wood, A.J., Wollenberg, B.F.: 'Power generation, operation, and control'. (John Wiley & Sons, 2012)

2 Abur, A., Exposito, A.G.: 'Power system state estimation: theory and implementation'. (CRC Press, 2004)

3 Schweppe, F.C.: 'Power system static-state estimation, part III: Implementation', *IEEE Trans Power App syst*, 1970, , (1), pp. 130–135

4 Huang, Y.F., Werner, S., Huang, J., Kashyap, N., Gupta, V.: 'State estimation in electric power grids: Meeting new challenges presented by the requirements of the future grid', *IEEE Signal Proc Mag*, 2012, **29**, (5), pp. 33–43

5 Boyd, S., Vandenberghe, L.: 'Convex optimization'. (Cambridge university press, 2004)

6 Kucuksari, S., Karady, G.G.: 'Experimental comparison of conventional and optical current transformers', *IEEE Transactions on power delivery*, 2010, **25**, (4), pp. 2455–2463

7 Kusic, G., Garrison, D. 'Measurement of transmission line parameters from scada data'. In: IEEE PES Power Systems Conference and Exposition, 2004. (IEEE, 2004. pp. 440–445

8 Irving, M., Owen, R., Sterling, M. 'Power-system state estimation using linear programming'. In: Proc. Inst. Elect. Eng.. vol. 125. (, 1978. pp. 879–885

9 Kotiuga, W.W., Vidyasagar, M.: 'Bad data rejection properties of weighted least absolute value techniques applied to static state estimation', *IEEE Trans Power App Syst*, 1982, , (4), pp. 844–853

10 Abur, A., Celik, M.K.: 'A fast algorithm for the weighted least absolute value state estimation (for power systems)', *IEEE Trans Power Syst*, 1991, **6**, (1), pp. 1–8

11 Celik, M.K., Abur, A.: 'A robust WLAV state estimator using transformations', *IEEE Trans Power Syst*, 1992, **7**, (1), pp. 106–113

12 Zhang, Y., Madani, R., Lavaei, J.: 'Conic relaxations for power system state estimation with line measurements', *IEEE Trans Control Network Syst*, 2018, **5**, (3), pp. 1193 – 1205

13 Wang, G., Zamzam, A.S., Giannakis, G.B., Sidiropoulos, N.D.: 'Power system state estimation via feasible point pursuit: Algorithms and cramer-rao bound', *IEEE Trans Signal Proc*, 2018, **66**, (6), pp. 1649–1658

14 Giannakis, G.B., Zhu, H.. 'State estimation of electrical power networks using semidefinite relaxation'. (Google Patents, 2018. US Patent 9,863,985

15 Jiang, X.T., Fardanesh, B., Maragal, D., Stefopoulos, G., Chow, J.H., Razanousky, M. 'Improving performance of the non-iterative direct state estimation method'. In: Power and Energy Conference at Illinois (PECI), 2014. (IEEE, 2014. pp. 1–6

16 Jiang, X.T., Chow, J.H., Fardanesh, B., Maragal, D., Stefopoulos, G., Razanousky, M.: 'Power system state estimation using a direct non-iterative method', *Int Jour Electr Power & Energy Syst*, 2015, **73**, pp. 361–368

17 Phadke, A.G., Thorp, J.S.: 'Synchronized phasor measurements and their applications'. (Springer Science & Business Media, 2008)

18 Phadke, A.G., Thorp, J.S., Karimi, K.: 'State estimation with phasor measurements', *IEEE Trans Power Syst*, 1986, **1**, (1), pp. 233–238

19 Yang, T., Sun, H., Bose, A.: 'Transition to a two-level linear state estimator-part II: Algorithm', *IEEE Trans Power Syst*, 2011, **26**, (1), pp. 54–62

20 Jones, K.D., Thorp, J.S., Gardner, R.M. 'Three-phase linear state estimation using phasor measurements'. In: Power and Energy Society General Meeting (PES). (IEEE, 2013. pp. 1–5

21 Dopazo, J., Klitin, O., Stagg, G., Van.Slyck, L.: 'State calculation of power systems from line flow measurements', *IEEE Trans power App Syst*, 1970, , (7), pp. 1698–1708

22 Porretta, B., Dhillon, R.: 'Performance evaluation of state estimation from line flow measurements on ontario hydro power system', *IEEE Trans Power App Syst*, 1973, , (5), pp. 1702–1712

23 Nuqui, R., Phadke, A.G. 'Hybrid linear state estimation utilizing synchronized phasor measurements'. In: Power Tech, IEEE Lausanne. (, 2007. pp. 1665–1669

24 Chakrabarti, S., Kyriakides, E., Ledwich, G., Ghosh, A.: 'Inclusion of PMU current phasor measurements in a power system state estimator', *IET gene, transm & distrib*, 2010, **4**, (10), pp. 1104–1115

25 Valverde, G., Chakrabarti, S., Kyriakides, E., Terzija, V.: 'A constrained formulation for hybrid state estimation', *IEEE Trans Power Syst*, 2011, **26**, (3), pp. 1102–1109

26 Gol, M., Abur, A.: 'LAV based robust state estimation for systems measured by PMUs', *IEEE Trans Smart Grid*, 2014, **5**, (4), pp. 1808–1814

27 Dobakhshari, A.S., Azizi, S., Paolone, M., Terzija, V.: 'Ultra fast linear state estimation utilizing SCADA measurements', *IEEE Trans Power Syst*, 2019, **34**, (4), pp. 2622–2631

28 'Matpower: A matlab power system simulation package'. (http://www.pserc.cornell.edu/matpower/,

29 'Power systems test case archive. Univ. of Washington.'. (http://www.ee.washington.edu/research/pstca.,
30 Caro, E., Conejo, A.J., Mínguez, R., Zima, M., Andersson, G.: 'Multiple bad data identification considering measurement dependencies', *IEEE Trans Power Syst*, 2011, **26**, (4), pp. 1953–1961
31 Zhao, J., Mili, L.: 'Vulnerability of the largest normalized residual statistical test to leverage points', *IEEE Trans Power Syst*, 2018, **33**, (4), pp. 4643 – 4646
32 Liu, Y., Ning, P., Reiter, M.K.: 'False data injection attacks against state estimation in electric power grids', *ACM Trans Inform and Syst Security (TISSEC)*, 2011, **14**, (1), pp. 21–32